


Atom-in-jellium predictions of the shear modulus at high pressure

Damian C. Swift ^{*}, Thomas Lockard, Sebastien Hamel, Christine J. Wu, Lorin X. Benedict, and Philip A. Sterne
Lawrence Livermore National Laboratory, 7000 East Avenue, Livermore, California 94551, USA



(Received 1 September 2021; revised 15 November 2021; accepted 13 January 2022; published 25 January 2022)

Atom-in-jellium calculations of the Einstein frequency in condensed matter and of the equation of state were used to predict the variation of shear modulus from zero pressure to $\sim 10^7$ g/cm³, for several elements relevant to white dwarf stars and other self-gravitating systems. This is by far the widest range reported electronic structure calculation of shear modulus, spanning from ambient through the one-component plasma to extreme relativistic conditions. The predictions were based on a relationship between the Debye temperature and shear modulus, which we assess to be accurate at the $o(10\%)$ level, and is the first known use of atom-in-jellium theory to calculate a shear modulus. We assessed the overall accuracy of the method by comparing with experimental measurements and more detailed electronic structure calculations at lower pressures.

DOI: [10.1103/PhysRevB.105.024110](https://doi.org/10.1103/PhysRevB.105.024110)

I. INTRODUCTION

The shear modulus is a fundamental measure of the resistance of matter to shear deformation, dictating the speed of propagation of shear waves, contributing to the speed of longitudinal waves, and governing the magnitude of deviatoric stresses induced by shear strains, which are the driving force for plastic flow. Although straightforward to measure at ambient pressure, the shear modulus is challenging to measure at elevated pressures because of the difficulty of distinguishing its contribution from that of the bulk modulus, i.e. volumetric compression of the sample. However, the shear modulus is a key aspect in understanding the response of solids to deformation at high pressure, which is typically dynamic. It represents the first-order correction to the scalar equation of state (EOS) to account for nonhydrostatic stresses. Technologically, the high-pressure shear modulus is important in impacts and the response of solids to explosions, as occur in weapon physics and target response. Scientifically, it occurs in planetary seismology and oscillatory modes of white dwarf and neutron stars—at very different pressure regimes.

The shear modulus is usually predicted theoretically from electronic structure calculations of single-crystal elastic moduli, which are then averaged to estimate the shear modulus of polycrystalline matter [1]. This approach is rigorous, but it is subject to some difficulties in practice. If the appropriate crystal structure is not represented accurately enough in the electronic structure model, or contains internal degrees of freedom for which the equilibrium parameter values are not found precisely enough, the model of the crystal may be unstable with respect to some distortions from the supposed equilibrium, giving unphysical negative elastic moduli. Because calculations of the elastic moduli usually break symmetries of the equilibrium structure, and several distortions of the structure are needed to determine the elastic moduli, the

computational effort involved is higher than for the EOS. For these reasons, predictions of elastic moduli are generally less extensive than are EOS.

Although single-crystal elastic properties are important for some applications, most require a polycrystalline average shear modulus. The properties of a polycrystalline ensemble depend on the texture of the material, which introduces another degree of freedom. The limiting cases of Voigt and Reuss averaging—assuming that either the stress or strain is equal over grains of different orientation—may be significantly different [2].

We present a different and computationally efficient method of predicting the shear modulus over a wide range of states, avoiding most of these complications. This method can be made to work with any approach to constructing the EOS from which the ion-thermal contribution can be identified. Here we use the atom-in-jellium method [3,4], which we have recently been investigating as a particularly efficient approach to predicting the EOS of elements over a wide range of states [5,6]. In fact, we have found it possible to calculate the EOS over eleven decades in mass density and ten in temperature, the first application of a reasonably accurate electronic structure technique to span from ambient conditions to the core of a white dwarf (WD) star [7]. The EOS and shear modulus predictions may be relevant to the study of the internal structure of WDs by asteroseismology and to gamma ray bursts from crustal quakes in magnetars.

II. RELATION BETWEEN SHEAR MODULUS AND ION-THERMAL EOS

Although it is considered most natural to express the ion-thermal EOS of crystalline matter in terms of phonons, there is a close connection with the elastic moduli, as they give the frequencies of the acoustic modes. In the phonon approach, the thermal energy of each phonon mode has the Bose-Einstein form. The ion-thermal EOS can be found by integrating over all the phonon modes [8]. However, many of the phonon

^{*}dswift@llnl.gov

modes are similar, and in integrating over the population the details of any given mode become unimportant. It is common in constructing even recent, rigorous, multiphase EOS to express the ion-thermal contribution as a few effective Debye modes, or even a single mode. Average Debye modes can be estimated from the density of phonon states or from the elastic moduli. There is a one-to-one correspondence between elastic moduli and the speeds of longitudinal and shear waves. Depending on the details of the approach adopted, including the particular software implementation, there can be significant advantages in deriving the ion-thermal energy from the elastic moduli instead of phonon modes. Although elastic moduli are susceptible to numerical instabilities as mentioned above, phonon modes are usually even more susceptible, which can result in a proportion of modes with unphysical, complex frequencies, unless the assumed structure is at least metastable at the instantaneous state and the equilibrium positions of the atoms are found to sufficient precision. If the phonon modes are calculated by making finite displacements of ions from equilibrium, the symmetry of the crystal lattice is often reduced even more than by the distortions used to calculate elastic moduli. Phonon calculations often require the electron wave functions to be constructed over a supercell of the lattice, in order to reduce the effect of image displacements in a periodic representation. These constraints can make phonon calculations considerably more expensive than calculations of elastic moduli.

If the ion-thermal EOS is represented by a single Debye mode, it is naturally related to a single shear modulus. Compared to the calculation of the ion-thermal energy by considering longitudinal and shear wave speeds instead of elastic moduli, this approach is based on average wave speeds instead of the average energy, i.e., at least in principle calculating an average over all directions and polarizations of the elastic waves. There is a long history of relating the Debye temperature θ_D to the shear modulus [9–11], and this approach for predicting the ion-thermal energy is still in use [12]. Following Anderson [11],

$$\theta_D(\rho) = \frac{h}{k_B} \left(\frac{3N_A \rho}{4\pi \bar{A}} \right)^{1/3} \bar{u}, \quad (1)$$

where h and k_B are Planck's and Boltzmann's constants, respectively, N_A is Avogadro's number, \bar{A} is the mean atomic weight, the average wave speed

$$\bar{u} = \left(\frac{1/u_l^3 + 2/u_s^3}{3} \right)^{1/3}, \quad (2)$$

and the shear and longitudinal wave speeds are

$$u_s = \sqrt{\frac{G}{\rho}}, u_l = \sqrt{\frac{B + 4G/3}{\rho}}. \quad (3)$$

Relating the Debye temperature and the shear modulus relies on a hierarchy of approximations, in this case that the material is either elastically isotropic, or comprises a uniform distribution of grain orientations so as to give an isotropic average response and the shear modulus is the Hill average [11].

Conversely, the shear modulus G may be estimated from the Debye temperature θ_D and bulk modulus B . This calculation involves inverting the function $\theta_D(B, G)$, which we

performed numerically by bracketing and bisection, defining the bracket with factors β_1 and β_2 of B , where $\beta_1 \ll 1$ and $\beta_2 \gg 1$. Another approach has been to ignore either B or G and so make the expression for θ_D invertible [13]: $\theta_D \propto \rho^{1/3} \sqrt{G/\rho}$. A similar cubic relation has been used to relate the shear modulus to the elastic moduli rather than the Debye temperature, in cubic crystals [14]. As well as predicting the shear modulus for materials of interest using the complete equation, we assess the accuracy of the approximate solution.

III. ATOM-IN-JELLIUM EQUATION OF STATE

The atom-in-jellium (AJ) model [3] of electronic structure in matter provides a computationally efficient way to predict wide-ranging EOS models that provides B and θ_D and is thus convenient for making wide-range predictions of the shear modulus. For convenience, we summarize key aspects of the AJ model. The AJ model approximates condensed matter by considering a single atom surrounded by a medium comprising a constant positive charge density representing neighboring nuclei, and a compensating constant negative charge density representing the electrons associated with those nuclei: the ‘‘jellium.’’ Wave functions are calculated explicitly for the electrons associated with the nucleus, with radial symmetry over an otherwise empty spherical cavity in the jellium, of the Wigner-Seitz volume. This is a geometrically-simplified version of the muffin-tin model, in which the electron states are calculated within a polyhedral cavity with mirror boundary conditions. In Liberman's AJ model [3], the electron wave functions are represented with a spherical Bessel function basis set centered on the nucleus. The electronic wave functions are spinless but the Dirac Hamiltonian is used and so relativistic contributions to the kinetic energy are included, significant at high atomic number or extremely high compression or temperature. The Coulomb potential is calculated self-consistently with the electron wave functions at each density and temperature. The Kohn-Sham exchange functional is used and correlation is neglected. All electrons are treated explicitly, so the method does not suffer from the complications of pseudopotential approaches where the number of electrons subsumed into the pseudopotential must change over wide ranges of compression. At finite temperature, a fractional average occupation is used for each electron state, so the method is average-atom rather than considering populations of atoms with integer occupations of each state. Because of the simplified geometrical treatment of the local environment of the atom, AJ theory was originally considered to be appropriate for matter in the fluid-plasma regime at compressions and temperatures significantly above ambient. However, some researchers mistrusted the average-atom predictions of thermal ionization, which gave localized perturbations along the shock Hugoniot in comparison to Thomas-Fermi theory, suspecting that these effects would be less pronounced in real matter comprising a population of different, discrete states of excitation [15]. The AJ method was thus not adopted widely for predicting EOS, as it was considerably more expensive computationally than Thomas-Fermi theory. Recently, path integral Monte Carlo calculations gave predictions of the EOS and shock Hugoniot in the dense plasma regime which validated the AJ

calculations [5], demonstrating that the average-atom treatment with a simplified geometrical environment for the atom was adequate. Following its development for wide-ranging electronic structure predictions, AJ theory was extended [4] using perturbation theory to calculate the restoring force on the nucleus for displacements from the center of the cavity in the jellium, and hence the Einstein temperature θ_E for oscillations of the nucleus. θ_E was used to estimate the Debye temperature θ_D by equating the thermal energy or mean squared displacement. This approach can be used to predict the ion-thermal EOS in the solid state, using a generalized Debye model: a counterintuitive capability for an approach otherwise more appropriate for the dense fluid and plasma. We subsequently developed an approach to predict the reduction in ionic heat capacity from 3 to $3/2k_B$ per atom as the temperature increases above melting [6], making a more natural and complete link between AJ theory and the EOS in the fluid-plasma regime. The different methods of calculating θ_D from θ_E gave significantly different predictions of the shear modulus. We found that the displacement calculation gave results which, compared with a range of experimental data, theoretical predictions, and previous models for a variety of elements at pressures up to ~ 0.1 TPa, were systematically lower by a factor ~ 3 , whereas the energy calculation was more consistent, so we used the latter for all the results reported here.

The shear modulus is expected to be a function of both mass density ρ and temperature T . Strength models often express the shear and flow stress, G and Y , in terms of pressure p instead of ρ . However, most materials expand with temperature along an isobar, so $\partial G/\partial T|_\rho$ is typically smaller than $\partial G/\partial T|_p$, and so we prefer to consider $G(\rho, T)$. Unusually, the AJ calculation gives $\theta_D(\rho, T)$ [5], so it can be used to predict the temperature-dependence of G as well as the density dependence. Trial calculations indicated that the variation with T was not much greater than the numerical noise in the AJ solution for θ_D , and we do not consider it further here.

In order to study the limiting trends as the atoms are compressed closely enough for all the electrons to be unbound, the one-component plasma (OCP) limit, we based the shear modulus calculations on AJ EOS models of H, He, C, O, Ne, and Mg, constructed previously for WD studies [7]. The WD EOS calculations were performed to a mass density $\rho(10^7)$ g/cm³, which is four orders of magnitude higher than usual for general-purpose EOS [16,17], and a temperature 10^6 eV, an order of magnitude higher than usual. The shear moduli deduced are thus applicable at least in principle to WDs and the crust of neutron stars. We also calculated the shear modulus for Fe, as an intermediate- Z element of astrophysical importance whose strength has been relatively well studied. The Fe shear modulus was calculated from a standard-range AJ tabulation. The numerical solution of the AJ electron wavefunction must be performed at a finite, nonzero temperature. As discussed previously [5], the original AJ solver exhibited numerical problems at temperatures below 1 eV, which we circumvented by a modified method of solution, constructing EOS tabulated down to an arbitrary ~ 10 K, chosen to be lower than any application we were aware of for those EOS. For our WD EOS study [7], we tabulated the EOS down to an arbitrary 1 K, chosen to be below the cosmic background temperature

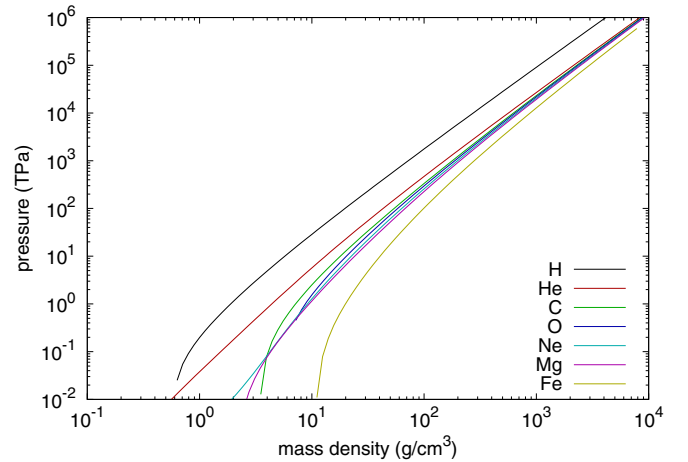


FIG. 1. 1-K isotherm from AJ calculation.

and thus lower than likely to be needed for any astrophysical application. Variations in the EOS below this level are very small, and far less than the inaccuracy in the AJ method. In all cases, B and θ_D were taken at the lowest temperature calculated in the AJ EOS, 1 K.

The pressure and bulk modulus were found to vary as $\rho^{5/3}$ at high compression, as expected for the OCP, and then tended toward $\rho^{3/2}$ in the extreme relativistic regime. These behaviors are a product of the AJ calculation, not imposed as an assumption. (Figures 1–3. Note that, when plotted over the full range calculated, the low pressure behavior is difficult to see, even on a logarithmic scale. Where we have truncated graphs at lower compressions than the full range calculated, the behavior beyond the upper limit follows the higher compression trend shown, without any noteworthy features. Data covering the full range are available online [18].)

The numerical solution of $G(B, \theta_D)$ performed reliably over the full range of densities considered, for all elements (Fig. 4). The simplified calculation neglecting B [13] gave results typically 30% higher.

The resulting $G(\rho)$ predictions were generated as tables. For convenience, we obtained functional fits to the tabular data: see Appendix.

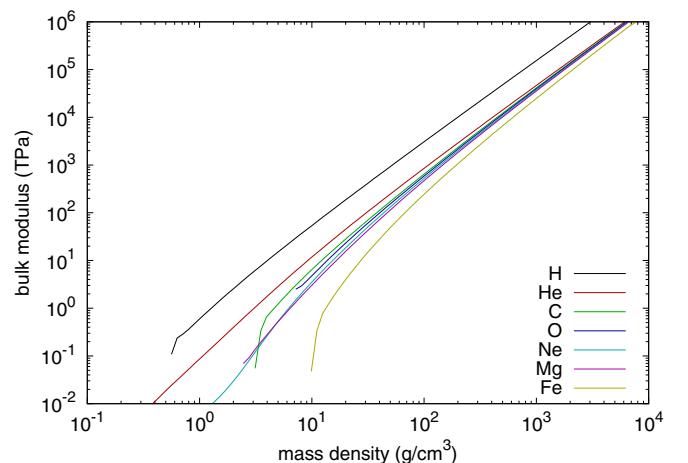


FIG. 2. Bulk modulus from AJ calculation.

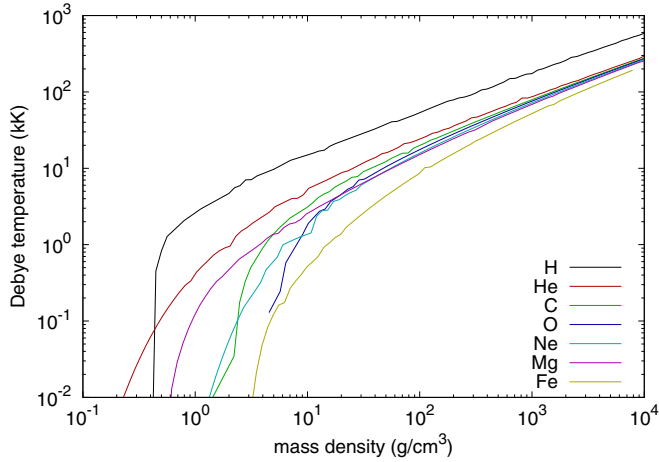


FIG. 3. Debye temperature from AJ calculation (from Einstein temperature by equating energy); (a) 1-K isotherm from AJ calculation. Bulk modulus from AJ calculation.

It is challenging to make EOS measurements at the terapascal range and above of materials that are solid at ambient conditions, and even more so to measure the shear modulus. For the elements considered here, our comparisons are primarily against ambient measurements where available, and otherwise against other models.

IV. PREVIOUS SHEAR MODULUS MODELS

Other models have been developed for the shear modulus at high pressure. We summarize three of them, Steinberg-Guinan, improved Steinberg-Guinan, and Straub, which are based at least partly on electronic structure theory, and for which results have been published for Mg, C, and Fe. We also contrast these models and the present approach with the Burakovsky-Greeff-Preston and finite strain models.

A. Steinberg-Guinan

The Steinberg-Guinan (SG) model [19] is widely used in hydrodynamic simulations below 100 GPa and has the form

$$G = G_0[1 + Ap/\eta^{1/3} - B(T - T_0)] \quad : \quad \eta \equiv \rho/\rho_0, \quad (4)$$

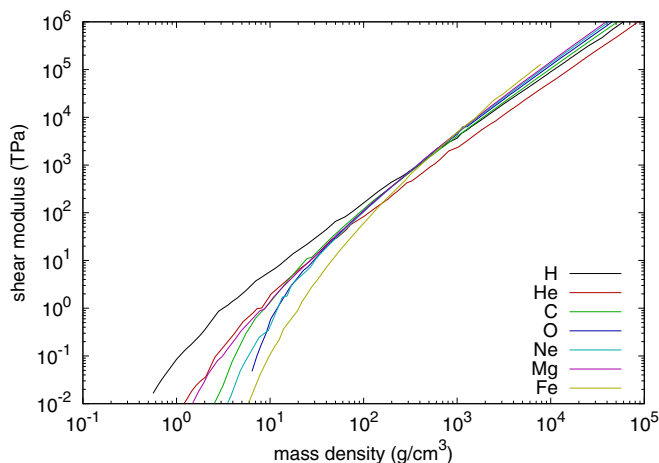


FIG. 4. Summary of AJ shear modulus predictions at 1 K.

where p is the pressure. Although developed for relatively low pressures, it is constructed to asymptote toward the compression-dependence of the one-component plasma (OCP) limit, where the shear modulus varies as $\rho^{4/3}$, if used in conjunction with a Thomas-Fermi like EOS model in which the pressure varies as $\rho^{5/3}$. However, the material-dependent parameters G_0 , A , and B are typically chosen to match low-pressure data, and the absolute value of G is not constrained to be correct in the OCP limit.

B. Improved Steinberg-Guinan

Improvements have been proposed to extend the SG model to higher pressures either by adopting different parameter values in high-pressure phases [20] or by modifying the dependence on compression to transition to a different function at high compressions [21]:

$$G = G_0\{f(\rho)G_l + [1 - f(\rho)]G_h - B(T - T_0)\}, \quad (5)$$

$$f(\rho) = \{1 + \exp[\alpha(\eta(\rho) - \eta_c)]\}^{-1}, \quad (6)$$

$$G_l = 1 + A_l p/\eta(\rho)^{1/3}, \quad (7)$$

$$G_h = A_h + M_h \eta(\rho), \quad (8)$$

$$\eta(\rho) = \rho/\rho_0. \quad (9)$$

Typically, the high pressure term G_h is calibrated against electronic structure calculations that extend into the terapascal range, but do not explore the OCP limit. Ironically, it is the low pressure term G_l that asymptotes to the expected OCP behavior, but is masked by the softer, linear dependence on ρ in G_h .

As the SG and improved SG (ISG) models depend on the pressure as well as the mass density, an EOS is needed when calculating the shear modulus. For consistency across all models, we used the AJ EOS. The AJ method is typically less accurate at pressures below a few tenths of a terapascal, so other models may appear to be less accurate at low pressures than used with alternative EOS.

C. Straub

In theoretical studies using early electronic structure predictions, it was observed that the variation of shear modulus G with the lattice parameter a in cubic crystals such as W behaves similarly to the bulk modulus $B(a)$. A similar form of fitting function was adopted as was used for the cold curve energy $E(a)$,

$$G = G_0 + g_a \frac{a - a_0}{a^2} e^{-g_2(a - a_0)}. \quad (10)$$

Parameters were fitted to electronic structure data points $\{a_i, G_i\}$ or to G_0 and $d \ln G/d \ln a$ [22]. Shear moduli have been predicted in this way for a small number of elements and included as tabulations of $G(\rho)$ in the SESAME library of material properties [16].

D. Burakovsky-Greeff-Preston

The Burakovsky-Greeff-Preston (BGP) model uses the density dependence of the Grüneisen parameter, the Lindemann melting law, and an approximate relationship between

shear modulus and the melting temperature $T_m(\rho)$,

$$G(\rho, T_m(\rho)) \propto \rho T_m(\rho), \quad (11)$$

to derive an expression for the shear modulus [23]:

$$G(\rho, T) = G(\rho_r, 0) \left(\frac{\rho}{\rho_r} \right)^{4/3} \exp \left\{ \sum_i \frac{2\gamma_i}{q_i} \left(\frac{1}{\rho_r^{q_i}} - \frac{1}{\rho^{q_i}} \right) \right\} \times \left(1 - \beta \frac{T}{T_m} \right). \quad (12)$$

As with the SG model, the BGP model is formulated explicitly to asymptote to the OCP-like $\rho^{4/3}$ behavior at high compression, and also like the SG model does not specify the magnitude in this limit independently of the dependence at low compressions. Parameters for the BGP model have not been reported for the elements considered here, though we have compared AJ predictions with BGP calibrations for other elements, with variable degrees of consistency [24]. We tried fitting the BGP model to our AJ predictions but were not able to obtain a wide-ranging match for any of the present set of elements.

E. Finite strain

“Finite strain” models have been developed for the pressure and shear modulus as a function of compression, particularly for materials of interest in planetary science [25,26]. This approach is based on making a Taylor expansion in pressure or compression about the ambient reference state, often constrained to asymptote to theoretically based behavior at high compression, such as Thomas-Fermi. The low-pressure behavior may be fitted to limited-range electronic structure calculations or empirical behavior such as that inferred from seismic wave propagation through the Earth; the problem here is that the precise composition of matter deep inside a planet is unknown. As has been recognized [25], adopting a low-order functional form that asymptotes to any given high-compression limit is unreliable as physical behavior at intermediate compressions—such as the compression-induced ionization of successive electron shells—is not captured.

V. DISCUSSION

The AJ method is known to be inaccurate at low pressure in comparison with multi-ion electronic structure techniques, and the derived calculation of shear modulus involves unquantified approximations. In particular, the AJ method does not account for angular forces such as occur in molecular bonds. It is interesting to compare with a recent analysis invoking the shear contribution to the longitudinal sound speed c_l in atomic matter, and comparing with high-fidelity electronic structure calculations of H [27]. c_l calculated from the AJ shear and bulk moduli agrees very well at low pressures with the theoretical analysis, to which multi-ion electronic structure calculations asymptote as H₂ molecules dissociate on compression. However, we find that c_l is dominated by the contribution from B for H in this regime, G being ~ 50 times smaller than B .

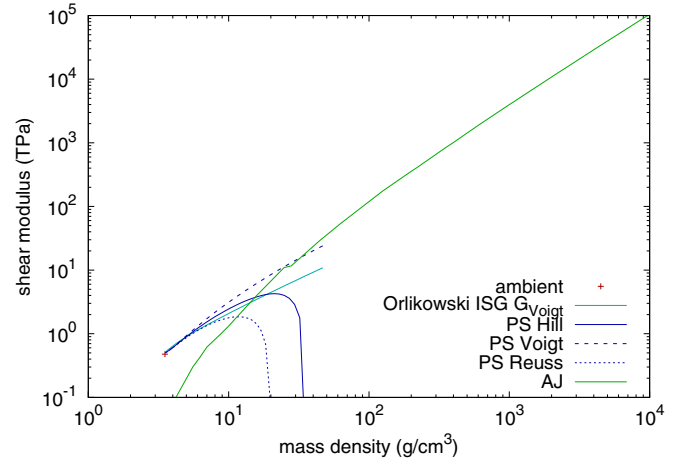


FIG. 5. Comparison of AJ shear modulus prediction with observed and calculated behavior for C, including pseudopotential based multi-ion calculations (PS) [2] and ISG model [21]. Pseudopotential predictions demonstrate possible range of shear modulus related to texture, and localized reductions in shear modulus associated with mechanical instability at a phase transition.

For C, the AJ shear modulus falls well below the observed value for diamond at STP, which is not surprising for a structure stabilized by directional bonding. The prediction passes through our recent pseudopotential predictions [2] above 10 g/cm³, crossing the Hill average just below 20 g/cm³ where the diamond structure was predicted to start to become unstable, and at higher compressions is more consistent with an extrapolation of the Voigt polycrystal average in diamond (Fig. 5).

For Mg, which adopts the hexagonal close-packed structure at low pressures, the AJ shear modulus reproduces the observed STP value to within a few percent. It follows the SG model quite closely over a wide pressure range. The SG model appears to have a discrepancy at low pressures; as discussed above, this is an artifact caused by using the AJ EOS to calculate the pressure, and is an example of better performance of electronic structure calculations in predicting derivatives of pressure than for the pressure itself [28]. The AJ prediction becomes quite close to the SG model above 10 g/cm³ (~ 1 TPa), and as the compression increases further, the AJ shear modulus gradually becomes a few tens of percent stiffer than the SG. The SG model in this regime is constrained only by its asymptotic form, and this result is an example of the SG model performing remarkably well. Mg exhibits solid-solid phase transitions [29,30], but the observed and predicted structures are close-packed structures or perturbations of simple structures stabilized by interactions between inner electrons at high pressures, and the AJ calculation is likely to be reasonable for bulk average mechanical properties (Fig. 6).

Fe exhibits solid phases, the low-pressure bcc structure being stabilized by magnetism, which the AJ model does not capture. The shear modulus of Fe at STP depends on the C content: low-C steels tend to be less rigid, and the AJ shear modulus lies relatively close to the lower reported values at STP. The Straub model is more consistent with C-rich Fe at low pressures, then passes through the AJ calculation around

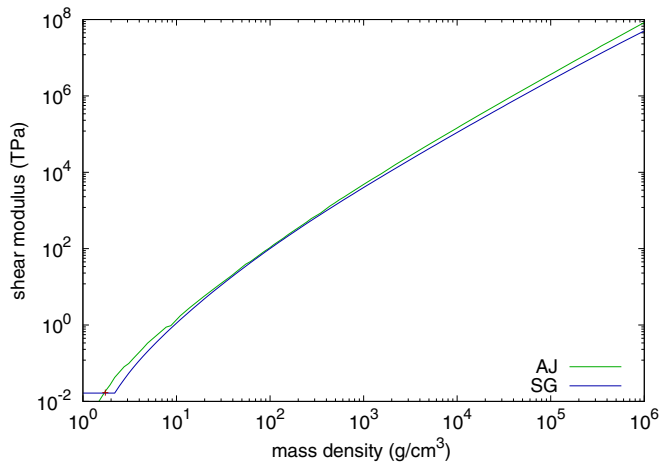


FIG. 6. Comparison of AJ shear modulus prediction for Mg with STP measurement and SG model.

4 TPa and lies well below at higher pressures. A SG calibration has been made for Fe at pressures of a few hundred gigapascals using multi-ion electronic structure calculations [31]. The AJ shear modulus intersects this model around 200 GPa and lies well below it at higher pressures. We suggest that these comparisons on balance favor the AJ calculation over a wide range of pressures (Fig. 7).

Shear modulus predictions based on multi-ion electronic structure are more accurate in principle than the AJ predictions presented here. However, in practice, differences in technique and the need to calculate and combine multiple elastic moduli mean that larger variations are commonly seen [2], and it has been difficult to generate wide-range predictions of shear modulus. Also, multi-ion calculations must be performed in a mechanically-stable phase, involving extra effort to identify an appropriate phase at each state. Dynamic loading experiments have commonly been performed outside the range of meaningful estimates of the shear modulus: this

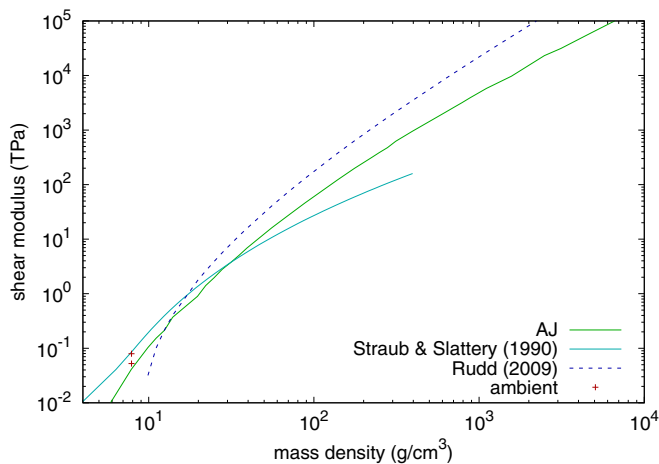


FIG. 7. Comparison of AJ shear modulus prediction for Fe with STP measurements and models, including the Straub model which is SESAME table 32140 [32] and the ISG model derived from multi-ion electronic structure calculations to the hundred gigapascal regime [31].

is no longer necessary for elements [33]. In high-pressure experiments, material strength is often a small effect in response dominated by the scalar EOS, and uncertainties $\sim 10\%$ in shear modulus appear correspondingly smaller in the overall response of the material. Because most materials are elastically anisotropic at some level, the effective shear modulus depends on the microstructural texture of the material, which may evolve during dynamic loading. Compared with microstructural effects (Fig. 5), an uncertainty $\sim 10\%$ is potentially insignificant.

VI. CONCLUSIONS

Shear moduli were predicted for condensed matter from zero pressure to beyond the OCP regime using predictions of the bulk modulus and θ_D from AJ theory. Although the predicted shear moduli are likely to be inaccurate for crystal structures stabilized by angular forces, which are not captured by AJ theory, they appear to be a reasonable choice over a wide range of compressions when a more rigorous model is not available. The likely accuracy of the shear modulus predictions reflects the uncertainties in the underlying methods: the approach adopted here could be used with more accurate treatments of electronic structure when the corresponding calculations of elastic moduli are not available, for instance for alloys and compounds.

Electronic structure calculations using the AJ method are often inaccurate around zero pressure, but appear to be accurate above a few hundred gigapascals, depending on the element. The method is valid to extreme relativistic conditions—beyond the OCP regime—of density and temperature. AJ does not capture crystal structures and directional bonding: it is likely to be inaccurate in low-pressure structures or around phase transitions, maybe by $\sim 100\%$. As with other pressure derivatives, the shear modulus otherwise seems to be predicted more accurately than the absolute pressure. Aside from numerical noise in the nuclear perturbation calculation, the calculation of θ_D is an approximate average. The inaccuracy may be of order 10%, though predicted trends are likely to be better.

The likely performance correlates with the crystal structure. Non-close-packed structures at low pressure are represented poorly in the AJ electron model, so the ion model and EOS are likely to be inaccurate. AJ typically fails to predict bound matter at the observed zero-pressure density. The shear modulus is then also likely to be inaccurate, except for fortuitous cancellations of error. Close-packed structures are captured reasonably in the AJ electronic model, particularly at elevated pressure, so the ion model and EOS are likely to be reasonable, as is the shear modulus. The performance is probably similar for amorphous and glassy structures. For lower-symmetry structures at high pressure, when these are perturbations to, or stacking faults in, close-packed structures, the quality of shear modulus predictions is likely to be similar to that for the close-packed structures. Open structures stabilized by strong directional bonds are likely to be less accurate. In unstable and mixed phases, the shear modulus may be small, which is not captured in the AJ predictions. The performance should not however be affected by whether a structure is metastable or not.

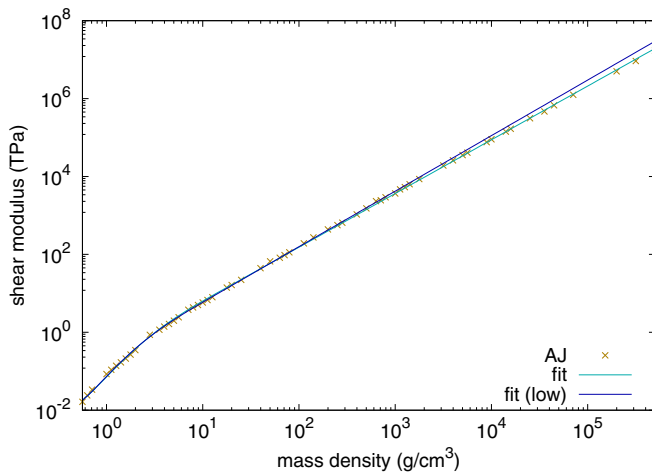


FIG. 8. Comparison of AJ shear modulus predictions for H with fits.

We have also developed a functional form capable of representing the AJ shear moduli over a wide range, although it is not valid over the full range of the AJ calculations.

ACKNOWLEDGMENTS

We thank the anonymous reviewers of this paper for their useful suggestions. This work was performed under the auspices of the U.S. Department of Energy under contract DE-AC52-07NA27344. G.J.A. would like to acknowledge funding from the ERC fellowship “Hecate” and from the EPSRC grant EP/P022790.

APPENDIX A: FIT TO AJ PREDICTIONS

We tried using existing strength models to fit the AJ shear modulus data, but did not manage to find parameter sets valid over the wide range of density of the AJ calculations. This is not to claim that reasonable fits are impossible to find, but fitting involves iterative optimization of parameters with a nonlinear dependence on the goodness of fit, which are often susceptible to numerical problems. A more general structure of model might involve a set of somewhat different functional

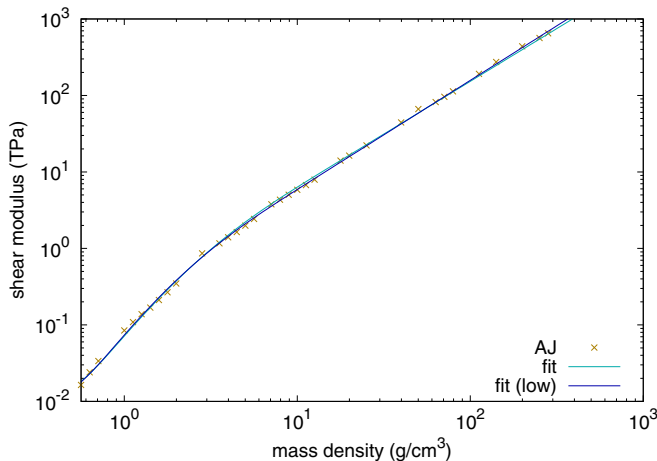


FIG. 9. Comparison of AJ shear modulus predictions for H with fits (detail at lower compression).

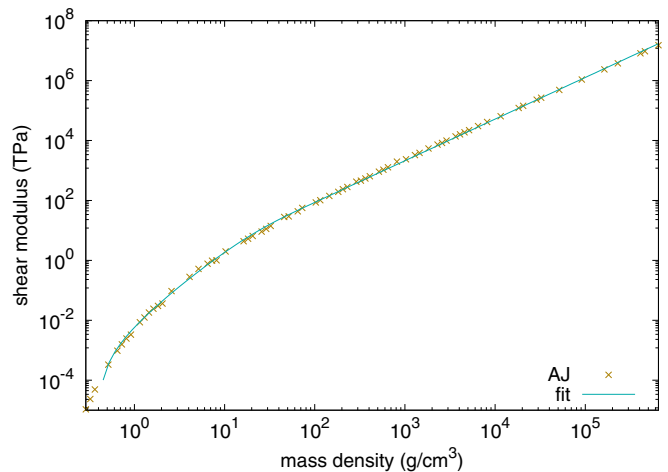


FIG. 10. Comparison of AJ shear modulus predictions for He with fit.

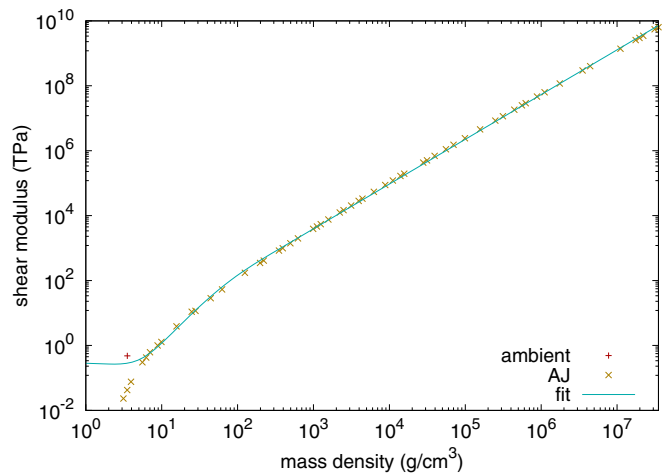


FIG. 11. Comparison of AJ shear modulus predictions for C with fit.

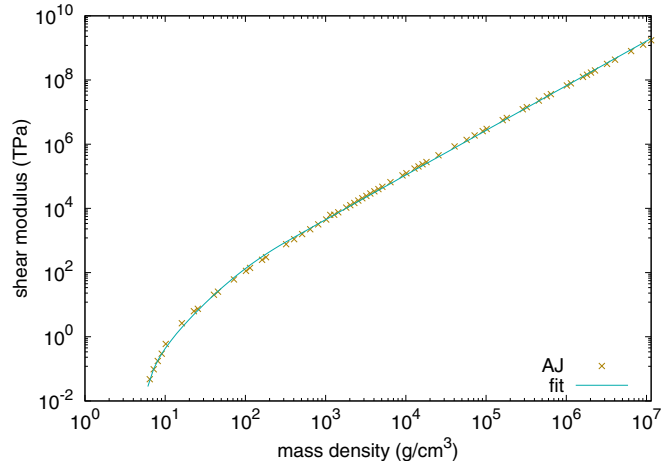


FIG. 12. Comparison of AJ shear modulus predictions for O with fit.

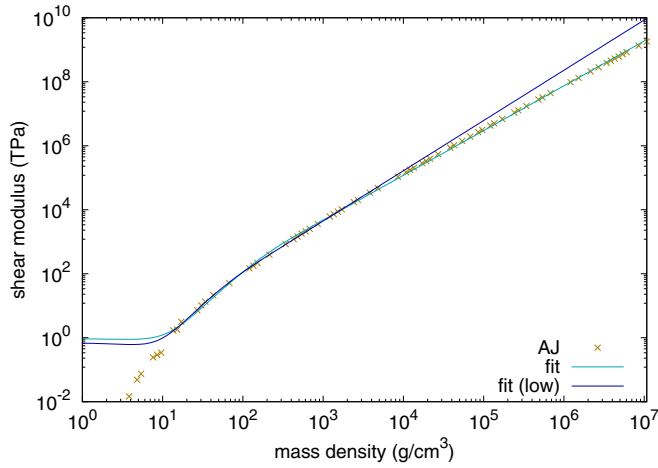


FIG. 13. Comparison of AJ shear modulus predictions for Ne with fit.

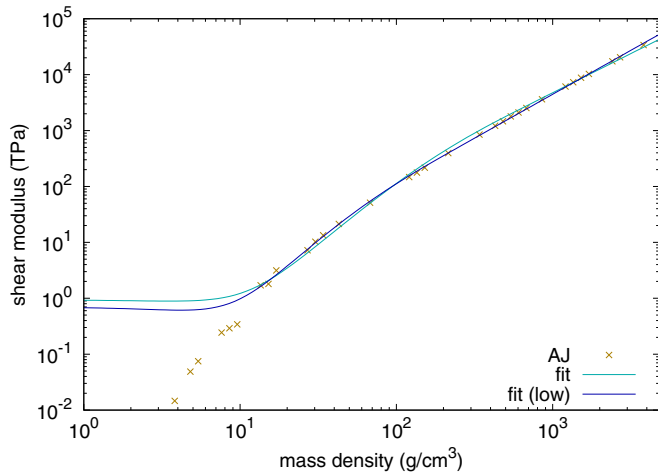


FIG. 14. Comparison of AJ shear modulus predictions for Ne with fits (detail at lower compression).

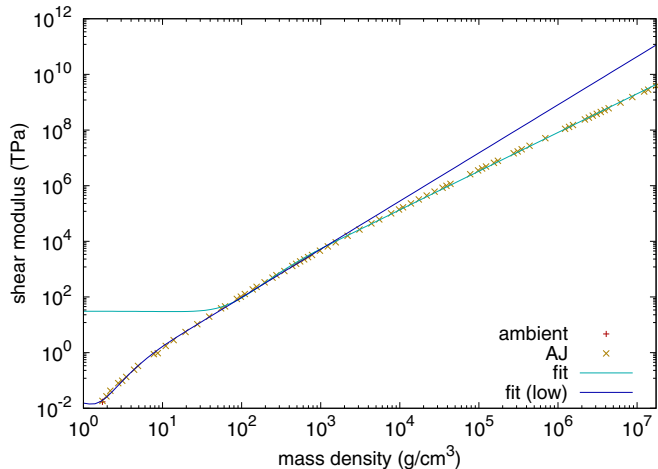


FIG. 15. Comparison of AJ shear modulus predictions for Mg with fits.

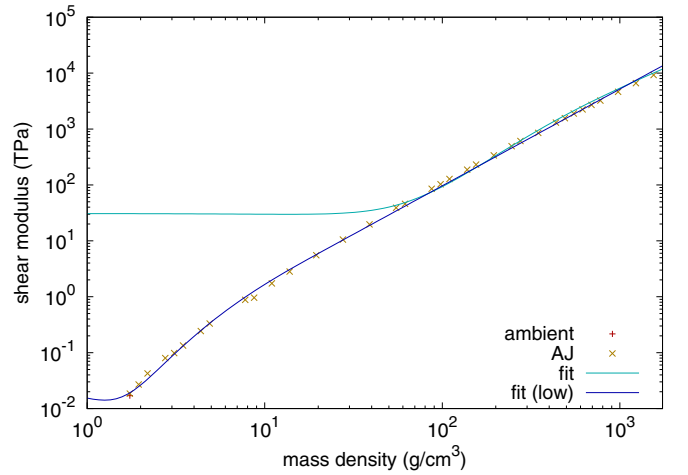


FIG. 16. Comparison of AJ shear modulus predictions for Mg with fits (detail at lower compression).

forms valid over restricted ranges of density, with a transition function between each, as in the ISG model for diamond [21]. We were unable to determine significant parameter values for a separate power dependence from the AJ shear modulus predictions at low density. Instead, reasonable fits were obtained using a single value at the reference density and the switching function itself to describe stiffening at low compression:

$$G(\rho) = G_0 f(\rho) + G_1 \left(\frac{\rho}{\rho_0} \right)^{p_1} [1 - f(\rho)], \quad (\text{A1})$$

where

$$f(\rho) = \exp\left(-\frac{\mu(\rho)}{\mu_t}\right) : \mu(\rho) \equiv \frac{\rho}{\rho_0} - 1, \quad (\text{A2})$$

and G_0 , G_1 , p_1 and μ_t are parameters. This functional form does not capture the AJ predictions in expansion, but this region is explored little in practice as materials spall in tension, limiting the distension of the bulk material. In general, this functional form does not represent the AJ shear modulus to the OCP regime with satisfactory accuracy at intermediate

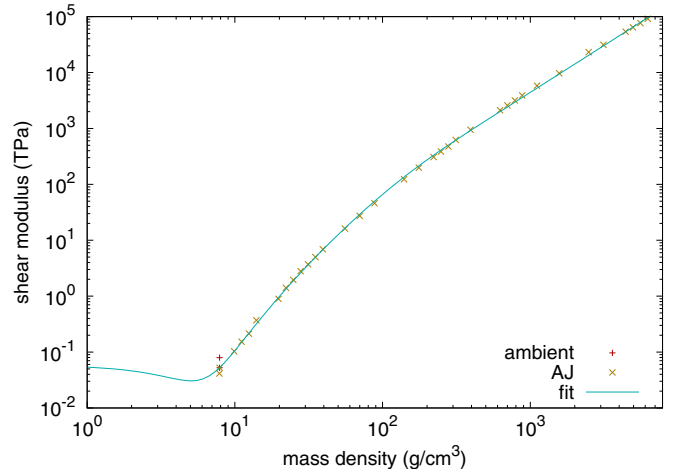


FIG. 17. Comparison of AJ shear modulus predictions for Fe with fit.

TABLE I. Fitting parameters for AJ shear modulus.

	ρ_0 (g/cm ³)	G_0 (GPa)	μ_t	G_1 (GPa)	p_1	Notes
H	0.5	14.5	3.0	82	1.43	$\geq \rho_0$, which is arbitrary, and ≤ 500 g/cm ³
H	0.5	15	3.9	103	1.379	$\geq \rho_0$, which is arbitrary, and $\leq 5 \times 10^5$ g/cm ³
He	0.5	0.3	26	55	1.390	≥ 2 g/cm ³ . ρ_0 is arbitrary. G_0 is consistent with zero
C	3.52	280	13	1.64×10^3	1.378	≥ 7 g/cm ³
O	6	24	11.6	3.6×10^3	1.392	$\geq \rho_0$, which is arbitrary
Ne	4.8	900	22	2.7×10^3	1.40	≥ 20 g/cm ³ . ρ_0 is arbitrary
Ne	4.8	600	7.3	1.0×10^3	1.57	for 12 to 5000 g/cm ³ , ρ_0 is arbitrary
Mg	1.738	3.0×10^4	140	8.0×10^2	1.39	≥ 100 g/cm ³
Mg	1.738	19	1.8	87	1.73	for 3 to 1000 g/cm ³
Fe	7.874	52.5	9.3	1.2×10^3	1.68	

compressions, so the exponent p_1 was included as a parameter in a finite-range fit (Table I.)

Where possible, the STP values of ρ and G were used as parameters, and low pressure AJ points were deweighted or removed if necessary. Otherwise, such as where AJ fails to capture solid phases with a significantly different shear modulus, the AJ data were fitted as far down in pressure as possible, G_0 was fitted if necessary, and ρ_0 was also adjusted if

needed to keep $G_0 > 0$. The resulting models are not intended for use at low pressure, though some are probably adequate for practical purposes.

The fitted equation usually matches the AJ data to within a few percent. Between numerical noise in the AJ calculation and probably-physical structure not captured by the equation, the deviation could be up to 20% in some places in most models and 30% in a few (Figs. 8–17).

[1] B. B. Karki, L. Stixrude, and R. Wentzcovitch, *Rev. Geophys.* **39**, 507 (2001).

[2] D. C. Swift, O. Heuzé, A. Lazicki, S. Hamel, L. X. Benedict, R. F. Smith, J. M. McNaney, and G. J. Ackland, [arXiv:2004.03071](https://arxiv.org/abs/2004.03071) [Phys. Rev. B (to be published)].

[3] D. A. Liberman, *Phys. Rev. B* **20**, 4981 (1979).

[4] D. A. Liberman and B. I. Bennett, *Phys. Rev. B* **42**, 2475 (1990).

[5] D. C. Swift, T. Lockard, R. G. Kraus, L. X. Benedict, P. A. Sterne, M. Bethkenhagen, S. Hamel, B. I. Bennett, *Phys. Rev. E* **99**, 063210 (2019).

[6] D. C. Swift, M. Bethkenhagen, A. A. Correa, T. Lockard, S. Hamel, L. X. Benedict, P. A. Sterne, and B. I. Bennett, *Phys. Rev. E* **101**, 053201 (2020).

[7] D. C. Swift, T. Lockard, S. Hamel, C. J. Wu, L. X. Benedict, P. A. Sterne, and H. D. Whitley, [arXiv:2103.03371](https://arxiv.org/abs/2103.03371).

[8] D. C. Swift, G. J. Ackland, A. Hauer, and G. A. Kyrala, *Phys. Rev. B* **64**, 214107 (2001).

[9] E. Madelung, *Physik. Zeitschrift* **11**, 898 (1910).

[10] A. Einstein, *Ann. Phys. (Leipzig)* **339**, 170 (1911).

[11] O. L. Anderson, *J. Phys. Chem. Solids* **24**, 909 (1963).

[12] For instance, H. K. Mao, J. Xu, V. V. Struzhkin, J. Shu, R. J. Hemley, W. Sturhahn, M. Y. Hu, E. E. Alp, L. Vocadlo, D. Alfè, G. D. Price, M. J. Gillan, M. Schwoerer-Böhning, D. Häusermann, P. Eng, G. Shen, H. Giefers, R. Lübbers, and G. Wortmann, *Science* **292**, 914 (2001); X. Liu and H.-Q. Fan, *R. Soc. Open Sci.* **5**, 171921 (2018).

[13] H. Ledbetter, *Z. Metallkd.* **82**, 820 (1991).

[14] E. Kröner, *Z. Phys.* **151**, 504 (1958).

[15] C. W. Greeff (private communication).

[16] S. P. Lyon and J. D. Johnson, Los Alamos National Laboratory report LA-UR-92-3407 (1992).

[17] D. A. Young and E. M. Corey, *J. Appl. Phys.* **78**, 3748 (1995).

[18] <https://gdo-hdp.llnl.gov/matprops/aj/>

[19] M. W. Guinan and D. Steinberg, *J. Phys. Chem. Solids* **35**, 1501 (1974).

[20] R. E. Rudd, L. H. Yang, P. D. Powell, P. Graham, A. Arsenlis, R. M. Cavallo, A. G. Krygier, J. M. McNaney, S. T. Prisbrey, B. A. Remington, D. C. Swift, C. E. Wehrenberg, and H.-S. Park, *Am. Inst. Phys. Conf. Proc.* **1979**, 070027 (2018).

[21] D. Orlikowski, A. A. Correa, E. Schwegler, and J. E. Klepeis, *Am. Inst. Phys. Conf. Proc.* **955**, 247 (2007).

[22] G. Straub, Los Alamos National Laboratory report LA-11806-MS (1990).

[23] L. Burakovsky, C. W. Greeff, and D. L. Preston, *Phys. Rev. B* **67**, 094107 (2003).

[24] D. C. Swift *et al.*, (unpublished).

[25] F. D. Stacey and P. M. Davis, *Phys. Earth Planet. Inter.* **142**, 137 (2004).

[26] A. Melinger-Cohen and R. Jeanloz, *J. Geophys. Res.: Solid Earth* **124**, 11651 (2019).

[27] K. Trachenko, B. Monserrat, C. J. Pickard, and V. V. Brazhkin, *Sci. Adv.* **6**, eabc8662 (2020).

[28] H. Akbarzadeh, S. J. Clark, and G. J. Ackland, *J. Phys.: Condens. Matter* **5**, 8065 (1993).

[29] C. J. Pickard and R. J. Needs, *Nat. Mater.* **9**, 624 (2010).

[30] P. Li, G. Gao, Y. Wang, and Y. Ma, *J. Phys. Chem. C* **114**, 21745 (2010).

[31] R. Rudd (private communication).

[32] G. Straub and W. Slattery, documentation for SESAME model 32140 (1990).

[33] D. C. Swift, Lawrence Livermore National Laboratory report LLNL-TR-814454 (2020), <https://gdo-hdp.llnl.gov/matprops/aj/shearfit.html>.